

A heuristic technique for CTIS image reconstruction

Michael D. Vose* and Mitchel D. Horton

Computer Science Department, University of Tennessee, Knoxville, Tennessee 37996, USA

*Corresponding author: vose@cs.utk.edu

Received 4 December 2006; revised 17 July 2007; accepted 24 July 2007;
posted 30 July 2007 (Doc. ID 77692); published 5 September 2007

An iterative method is presented for computed tomography imaging spectrometer (CTIS) image reconstruction in the presence of both photon noise in the image and postdetection Gaussian system noise. The new algorithm, which assumes the transfer matrix of the system has a particular structure, is evaluated experimentally with the result that it is significantly better, for larger problems, than both the multiplicative algebraic reconstruction technique (MART) and the mixed-expectation image-reconstruction technique (MERT) with respect to accuracy and computation time. © 2007 Optical Society of America
OCIS codes: 100.1830, 100.2000, 100.3020.

1. Introduction

Maximum-likelihood image reconstruction techniques are important tools in the restoration of noise corrupted images. They have widespread use in areas from imaging spectroscopy to emission tomography [1–3]. Our technique first removes noise via maximum-likelihood, and then subsequently performs image reconstruction by exploiting the particular structure of the matrix modeling the noise-free system. It is therefore specific to particular systems, like the computed-tomography imaging spectrometer (CTIS), whose noise-free system matrix may sometimes be acceptably approximated by one having the required structure. CTIS systems have wide ranging applications [4–10]; and have also received attention with respect to research directed at advancing their underlying technology [11–15]. This paper advances mathematical techniques for CTIS image reconstruction under frequently made assumptions.

A CTIS records spatial and spectral information about a scene by sampling a tomographic dispersion pattern formed by a computer generated hologram disperser [16]. A mathematical model describing the system is

$$g = Hf + n_1 + n_2, \quad (1)$$

where the transfer matrix H represents the optical processing of the CTIS system, g is the measured image obtained on the focal plane array, f is the object vector representing the flash hyperspectral image, and the n_i are noise terms.

Garcia and Dereniak [17] take n_1 to be Poisson distributed photon noise, and n_2 to be zero mean post-detection Gaussian system noise. They assume the standard deviation σ_s of n_2 is known, and that each Poisson distributed term $(Hf)_k + (n_1)_k$ is well approximated by a normal distribution with mean and variance $(Hf)_k$. Assuming statistical independence of all components g_m , they present an iterative technique to recover f from the measurement g , based on a maximum likelihood estimator.

This paper extends the results of Garcia and Dereniak in two ways. First, the result of their maximum likelihood estimator is obtained in explicit closed form, which transforms the stochastic problem (1) into a deterministic problem of the form

$$x = Hf. \quad (2)$$

Second, a heuristic method for recovering f from x is presented, which for larger problems is significantly better with respect to both accuracy and computational time (the object vector f used by Garcia and Dereniak [17] has 289 components; in our experiments f has 174,960 components). The improvement, however, comes at the cost of requiring the transfer

matrix H to have a “shift-invariant” structure. The precise details of that structure are explained after discussing noise removal, since noise removal does not rely upon any special structure.

Our technique is empirically tested in a noise-free and a noisy scenario, using a calibrated transfer matrix (calibration assumes shift-invariance to avoid the enormous inconvenience of measuring the point-spread function for every position in the field of view). In the latter case, both normal and Poisson noise are included in the data (as described above, with $\sigma_s = 2$), and we compare our results with those obtained from Garcia and Dereniak’s method [17].

2. Removing Noise

The assumptions described in the introduction imply that g_k is approximated by a normal random variable with mean $(Hf)_k$ and variance $\sigma_s^2 + (Hf)_k$. Using that approximation and assuming statistical independence of the components of g , the probability of measuring g given f is

$$\text{Prob}(g|f) = \prod_k \exp\left\{-\frac{(g_k - x_k)^2}{2x_k + 2\sigma_s^2}\right\} / \sqrt{2\pi(x_k + \sigma_s^2)}, \quad (3)$$

where $x = Hf$. This is essentially Garcia and Dereniak’s problem formulation [17]. Rather than basing an iterative technique on (3), we solve explicitly as follows.

Differentiating the logarithm of (3) with respect to x_k leads to the optimization condition

$$0 = \frac{(x_k + \sigma_s^2) - 2(g_k - x_k)(x_k + \sigma_s^2) - (g_k - x_k)^2}{(x_k + \sigma_s^2)^2}.$$

Since x_k is assumed to be a variance—of $(Hf)_k + (n_1)_k$ —it is the nonnegative root

$$x_k = \frac{\sqrt{(1 + 2\sigma_s^2)^2 + 4(g_k(g_k + 2\sigma_s^2) - \sigma_s^2)} - (1 + 2\sigma_s^2)}{2}. \quad (4)$$

In order that x_k is indeed nonnegative, it must happen that

$$g_k(g_k + 2\sigma_s^2) - \sigma_s^2 \geq 0,$$

and therefore

$$g_k \geq \sqrt{\sigma_s^4 + \sigma_s^2} - \sigma_s^2. \quad (5)$$

Hence by redefining g_k where necessary to ensure the above constraint (5), then $x = Hf$ may be regarded as known, it is obtained via (4), and it remains to determine f .

3. Recovering the Hyperspectral Image

A. Assumptions

Our heuristic method of obtaining an approximate solution to

$$x = Hf$$

is based on two assumptions concerning the structure of the $n \times m$ matrix H .

1. Assume the transfer matrix can be partitioned as

$$H = (H_0 | \cdots | H_{w-1}),$$

where each H_k is comprised of (the same number of) *rectangular* circulant blocks

$$H_k = (T_{k,0} | \cdots | T_{k,\alpha-1}),$$

(i.e., the i, j th entry of the *rectangular* matrix $T_{k,\ell}$ is some function of $i - j \bmod n$).

2. Assume each rectangular matrix $T_{k,\ell}$ is $n \times a$ (thus H has $m = a\alpha w$ columns), and

$$T_{k,\ell} = R_g^\ell T_{k,0},$$

where $g \geq a$, $n \geq \alpha g$, and R_g is the $n \times n$ circulant matrix

$$(R_g)_{i,j} = [g = i - j \bmod n].$$

Here the notation $[expression]$ denotes 1 if *expression* is true, and 0 otherwise.

It is known that the CTIS process is *not* shift-invariant [18–20], i.e., the second assumption above does not hold. However, past study has shown the assumption may yield a reasonable approximation [8–21], and the assumption is often taken for granted; one reads of “. . . the shift-invariance of the CTIS instrument . . .” [9] even though in general it cannot be well approximated by a shift-invariant system.

This paper does not explore the validity of that approximation, but considers instead the mathematical problem defined by equation (2) of recovering f from x based on assumptions frequently made for CTIS (noise removal was dealt with in the previous section). We are therefore concerned with advancing mathematical technique for CTIS image reconstruction based on a shift-invariant linear approximation of the system, rather than the nonlinear physical system itself.

B. Consequences of the Assumptions

Any $n \times n$ circulant matrix C is characterized by the existence of a vector c such that

$$C_{i,j} = c_{i-j \bmod n},$$

and thus is determined by its first column $c = Ce_0$, where e_0 is the first column of the identity matrix (a circulant matrix is differentiated from a *rectangular* circulant matrix by the requirement that a circulant matrix is square). Moreover, C is circulant if and only if $C = F^*DF$, where D is diagonal [in fact, $D = \sqrt{n} \text{diag}(Fc)$], F^* is the conjugate transpose of F , and F is the Fourier transform matrix

$$F_{i,j} = \frac{1}{\sqrt{n}} e^{2\pi\sqrt{-1}ij/n}.$$

These facts may be used to computational advantage when implementing our method, since the circulant matrices involved may be diagonalized (and computations may be conducted in the diagonalizing basis).

Define the $g \times a$ matrix Q by

$$Q = \begin{pmatrix} I_a \\ 0 \end{pmatrix},$$

where I_k is the $k \times k$ identity matrix. Let E be the $n \times \alpha a$ matrix

$$E = \begin{pmatrix} I_\alpha \otimes Q \\ 0 \end{pmatrix},$$

where \otimes denotes the Kronecker product [22]. It follows (by partitioning the vector f below) that

$$Hf = (H_0 | \cdots | H_{w-1}) \begin{pmatrix} f_0 \\ \vdots \\ f_{w-1} \end{pmatrix} = \sum H_k f_k = \sum C_k E f_k,$$

where C_k is the circulant matrix whose first column is that of $T_{k,0}$. This is a consequence of the equality $H_k w = C_k E w$ (for all k and any $\alpha a \times 1$ vector w), which is not difficult to verify using partitioned w . Define the partitioned matrix H by

$$H = (C_0 | \cdots | C_{w-1}).$$

It follows from the above that

$$x = Hf = H(I_w \otimes E)f. \tag{6}$$

C. Alternate Problem Formulation

One might therefore hope, on the basis of (6), that the system

$$\begin{aligned} h &= H^T x = H^T H y, \\ y &= (I_w \otimes E)f, \end{aligned} \tag{7}$$

is a reasonable alternative to $x = Hf$, since

$$f = (I_w \otimes E^T)y,$$

provided

$$y = (I_w \otimes E)(I_w \otimes E^T)y. \tag{8}$$

Attempting to solve (7) is problematic, however, for two reasons. First, $H^T H$ may be singular. Second, a solution y satisfying (7) might not satisfy (8).

D. Regularizing the Problem

The first difficulty, that $H^T H$ might not be invertible, is addressed by considering the regularized problem

$$h = (\mu I + H^T H)y,$$

which by the Sherman–Morrison–Woodbury identity [23],

$$(A + UCV)^{-1} = A^{-1} - A^{-1}U(C^{-1} + VA^{-1}U)^{-1}VA^{-1},$$

has the solution

$$y = (\mu^{-1}I - \mu^{-2}H^T(I + \mu^{-1}\sum C_k C_k^T)^{-1}H)h \tag{9}$$

(in our numerical experiments $\mu = 0.01$). What is particularly nice about this is that the matrix

$$I + \mu^{-1}\sum C_k C_k^T$$

is circulant, and therefore its inverse is trivial to compute: circulant matrices are closed under transpose, addition, multiplication, scaling (i.e., multiplication by scalars), powers, roots, and are trivially inverted (when nonsingular) [24].

E. Iterative Heuristic for the Regularized Alternate Problem

The second difficulty, that y computed by (9) need not satisfy (8), is dealt with in a heuristic manner as follows. Define the $nw \times nw$ matrix M and the $nw \times n$ matrix P by naming the right hand side of (9) to express it as

$$y = Mh = (\mu^{-1}I - PP^T)h,$$

and note that since $M = (\mu I + H^T H)^{-1} = \mu^{-1}I - PP^T$ it follows that

$$MH^T H = \mu PP^T, \tag{10}$$

where

$$P = \mu^{-1}H^T(I + \mu^{-1}\sum C_k C_k^T)^{-1/2}.$$

Equation (10) will be used below. Let $Z' = I - Z$, where Z is defined as

$$Z = \text{diag}((I_w \otimes E)\mathbf{1}_m),$$

and where $\mathbf{1}_m$ is the $m \times 1$ vector all of whose entries are 1. Define the vectors \tilde{y}_i and \tilde{v}_i as follows (since these vectors have subscripted names, they are decorated with “hats” so as to distinguish them from scalars):

$$\begin{aligned}\tilde{y}_0 &= ZMh & \tilde{y}_{i+1} &= \tilde{y}_i + ZMH^T H\tilde{v}_i, \\ \tilde{v}_0 &= Z'Mh & \tilde{v}_{i+1} &= Z'MH^T H\tilde{v}_i.\end{aligned}$$

It follows from (10) and the recursive equations above that

$$\begin{aligned}\tilde{y}_\infty &= \lim_{i \rightarrow \infty} \tilde{y}_i \\ &= ZMh + \mu ZPP^T \sum_{i=0}^{\infty} \{\mu(Z'P)(Z'P)^T\}^i \tilde{v}_0 \\ &= Z(I + \mu PP^T \{I - \mu(Z'P)(Z'P)^T\}^{-1} Z')Mh.\end{aligned}$$

Applying the Sherman–Morrison–Woodbury formula to the inverse occurring in the last expression above yields

$$\tilde{y}_\infty = Z(I + \mu PP^T Z' \{I + P(\mu^{-1}I - P^T Z'P)^{-1} P^T Z'\})Mh. \quad (11)$$

Note that evaluating \tilde{y}_∞ requires *only* that the inverse $(\mu^{-1}I - P^T Z'P)^{-1}$ can be multiplied by vectors on the right. Hence products of the form

$$(\mu^{-1}I - P^T Z'P)^{-1}v$$

can be obtained by applying a conjugate gradient method [23] to solve

$$v = (\mu^{-1}I - P^T Z'P)u. \quad (12)$$

The first step in our heuristic method is to take the first approximation \tilde{f}_0 to solving $x = Hf$ as

$$\tilde{f}_0 = (I_w \otimes E^T)\tilde{y}_\infty,$$

where \tilde{y}_∞ is determined by (11) subject to the condition that the embedded conjugate gradient method, which solves expressions of the form (12), is terminated at the first local minimum of error [in solving (12); see Appendix] or at LIM number of conjugate gradient steps (LIM is a parameter, typically chosen less than 5).

Subsequent steps in our heuristic method proceed as follows. Let the vectors produced by previous steps be

$$\tilde{f}_0, \dots, \tilde{f}_i$$

and let

$$\sum \eta_i \tilde{f}_i$$

be the least-squares solution [23] to minimizing $\|x - H\sum \eta_i \tilde{f}_i\|$. Obtain \tilde{f}_{i+1} in the same manner as \tilde{f}_0 ,



Fig. 1. Initial field of view image f : closeup of mosquito.

except with respect to the problem

$$x - H \sum \eta_i \tilde{f}_i = Hf.$$

4. Experimental Results

We used a 4194304×174960 shift-invariant matrix $H = (H_0 | \dots | H_{23})$ corresponding to a calibrated CTIS system. Each H_i has 90 rectangular circulant blocks, each of which is 4194304×81 . Whereas f would typically be interpreted as encoding 24 images of the same object at various wavelengths, that interpretation is completely artificial and totally irrelevant to the mathematical problem which is represented by Eq. (1). The image recovery problem this paper is concerned with has the following pertinent characteristics:

- Information goes in, as represented by some vector f .
- That information becomes encoded in the vector $g = Hf + n_1 + n_2$.
- One attempts to recover the original information f from the encoding g .

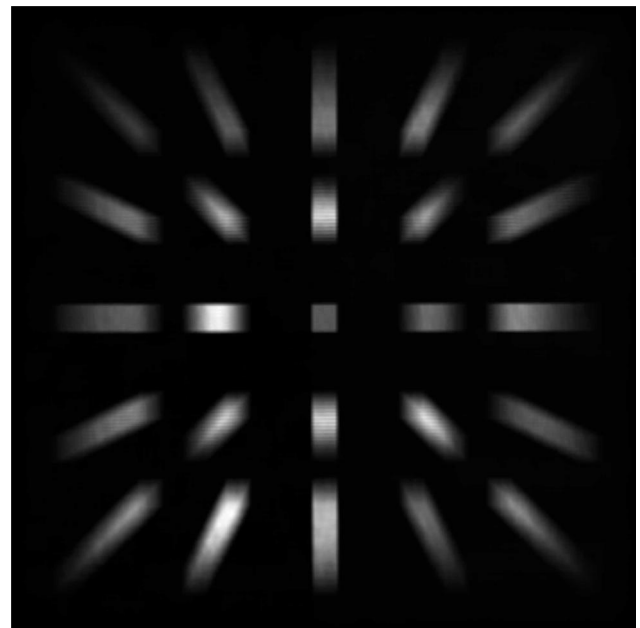


Fig. 2. CTIS focal plane image g (corresponding to f).

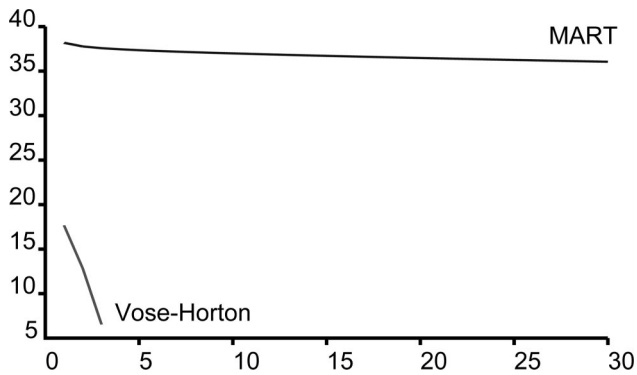


Fig. 3. Average pixel error versus iteration.

It serendipitously happens that there are a total of $24 \times 90 \times 81 = 174960$ components of f , exactly enough to accommodate a 324×180 color (pulse-position-modulation signal) (PPM) image (PPM format specification: <http://netpbm.sourceforge.net/doc/ppm.html>). For purposes of evaluating our method, this interpretation of f , as a single 324×180 color PPM image, is far superior to dealing with 24 monochromatic images (each 90×81 pixels) because they would be much too small to realistically portray a complicated image suitable to visually demonstrate the power of our method. The PPM image we used for f is a close-up of a mosquito (Fig. 1). The corresponding CTIS focal plane image g is given in Fig. 2.

Figure 3 corresponds to the noise-free case. It shows average pixel error plotted against iterations for the following methods:

- Multiplicative algebraic reconstruction technique (MART) [6].
- Vose–Horton (our heuristic method).

Average pixel error is the average over all components of the absolute deviation between the image (i.e., components of f) and the recovered image (i.e., components of the approximate solution s to $g = Hs$ as computed by the image reconstruction techniques).

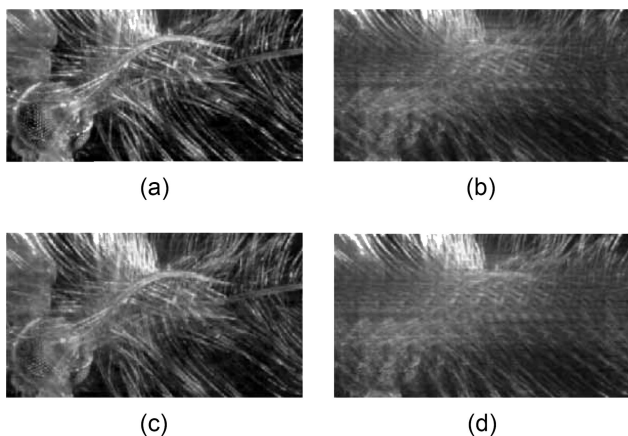


Fig. 4. (a) Vose–Horton (3 iterations; 457 s); (b) MART (3000 iterations; 45700 s); (c) Vose–Horton (4 iterations, noise level $\sigma_s = 2$; 470 s); (d) MERT (210 iterations, noise level $\sigma_s = 2$; 4700 s).

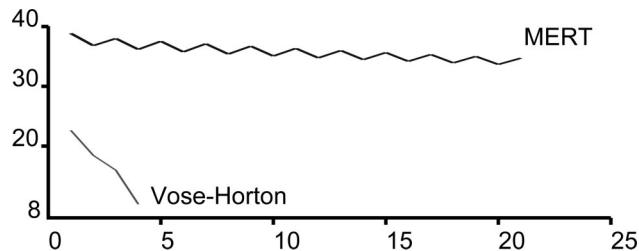


Fig. 5. Average pixel error versus iteration (noise level $\sigma_s = 2$).

The meaning of iteration for MART is a transition from the current to the next estimate:

$$f^{k+1} = f^k \frac{H^T g + \mu \mathbf{1}}{H^T H f^k + \mu \mathbf{1}},$$

where $\mathbf{1}$ is the vector of all 1 s, and the regularization parameter μ is either zero (no regularization) or 0.01 (regularization). The meaning of iteration for our method is a step as described in the previous section, with LIM = 4. Since an iteration of Vose–Horton takes longer than an iteration of MART, *both methods were run for an equal amount of time* (457 seconds executing on a gentoo gnu/linux dual-socket dual-core amd64 workstation), which corresponds to 30 iterations for MART, and 3 iterations for Vose–Horton.

Figure 4(a) and 4(b) show the reconstructed images, except there the image for MART corresponds to 3000 iterations, demonstrating that *given two orders of magnitude more time than taken by Vose–Horton, MART is only beginning to converge*. It is interesting that regularization had no significant effect (the initial components of f^0 were set to the average component value of f).

Figure 5 corresponds to the case where noise corrupts the image. As was done by Garcia and Dereniak [17], we take $\sigma_s = 2$. Our method (with LIM = 4) is compared with the mixed-expectation image-reconstruction technique (MERT) [17]. *Both methods were run for an equal amount of time* (470 seconds), which corresponds to 21 iterations for MERT, and 4 iterations for Vose–Horton.

Figures 4(c) and 4(d) show the reconstructed images, except there the image for MERT corresponds to 210 iterations, demonstrating that *given an order of magnitude more time than taken by Vose–Horton, MERT is only beginning to converge*.

In our experiments, both MART and MERT do eventually converge, but to produce results comparable with Vose–Horton, MART takes three orders of magnitude (10^3) more time, and MERT takes two orders of magnitude (10^2) more time.

5. Conclusion

We present a new algorithm for reconstructing the data cube from the focal plane image captured by a computed-tomography imaging spectrometer (CTIS) [16]. Our method is specialized in that it assumes the

transfer matrix of the system has a shift-invariant structure. An empirical evaluation demonstrates that, for larger problems, our method is a significant improvement over both MART and MERT with respect to accuracy and computation time.

Appendix

The following iterative scheme to compute a solution to $Ax = b$ (where A is symmetric positive definite, and the notation (\cdot, \cdot) in the algorithm below denotes inner product) is what we mean by a “conjugate gradient” method:

```
x = initial
p = r = b - Ax
e = (r, r)
while (e > epsilon) {
    v = Ap
    a = e/(p, v)
    x = x + a*p
    r = r - a*v
    a = (r, r)
    p = r + (a/e)*p
    e = a
}
```

The definition of “local minimum of error” (referred to in the description of our method) is the first local minimum in the sequence e_1, e_2, e_3, \dots , where e_i is the value of the variable e at the i th iteration of the while loop in the code above.

We are pleased to acknowledge helpful conversations with Dr. Jacob Barhen, director of the Center for Engineering Science Advanced Research (CESAR) at the Oak Ridge National Laboratory (ORNL). This work was supported by The University of Tennessee Science Alliance in conjunction with ORNL LDRD.

References

1. H. H. Barrett, “Image reconstruction and the solution of inverse problems in medical imaging,” in *The Formation, Handling, and Evaluation of Medical Images*, A. Todd-Pokropek and M. A. Viergever, eds. (Springer-Verlag, 1991), pp. 33–39.
2. T. R. Miller and J. W. Wallis, “Clinically important characteristics of maximum-likelihood reconstruction,” *J. Nucl. Med.* **33**, 1678–1684 (1992).
3. M. R. Descour, “Non-scanning imaging spectrometry,” Ph.D. dissertation (University of Arizona, 1994).
4. M. R. Descour, B. K. Ford, D. W. Wilson, P. D. Maker, and G. H. Bearman, “High-speed spectral imager for imaging transient fluorescence phenomena,” *Proc. SPIE* **3259**, 11–17 (1998).
5. C. E. Volin, J. P. Garcia, E. L. Dereniak, M. R. Descour, T.

- Hamilton, and R. McMillan, “Midwave-infrared snapshot imaging spectrometer,” *Appl. Opt.* **40**, 4501–4506 (2001).
6. B. K. Ford and M. R. Descour, “Large-image-format computed tomography imaging spectrometer for fluorescence microscopy,” *Opt. Express* **9**, 444–453 (2001).
7. B. Karacali and W. Snyder, “Automatic target detection using multispectral imaging,” presented at the 31st Applied Imagery Pattern Recognition Workshop, 16 October 2002, Washington, DC, p. 55.
8. E. K. Hege, D. O’Connell, W. Johnson, S. Bastys, and E. L. Dereniak, “Hyperspectral imaging for astronomy and space surveillance,” *Proc. SPIE* **5159**, 380–391 (2003).
9. M. R. Descour, T. S. Tkaczyk, B. K. Ford, R. M. Lynch, A. Locke, and E. L. Dereniak, “The computed tomography imaging spectrometer,” in *The 16th Annual Meeting of the IEEE Lasers and Electro-Optics Society, 2003. LEOS 2003* (IEEE, 2003), pp. 460–461.
10. W. R. Johnson, D. W. Wilson, W. Fink, M. Humayun, and G. Bearman, “Snapshot hyperspectral imaging in ophthalmology,” *J. Biomed. Opt.* **12**, 014036 (2007).
11. N. Hagen, E. L. Dereniak, and D. T. Sass, “Development of a four-dimensional imaging spectrometer,” *Proc. SPIE* **4816**, 381–388 (2002).
12. J. F. Scholl, E. L. Dereniak, M. R. Descour, C. P. Tebow, and C. E. Volin, “Phase grating design for a dual-band snapshot imaging spectrometer,” *Appl. Opt.* **42**, 3745–3748 (2003).
13. N. Hagen, E. L. Dereniak, and D. T. Sass, “Visible snapshot imaging spectropolarimeter,” *Proc. SPIE* **5888**, 277–286 (2005).
14. N. Hagen and E. L. Dereniak, “Design of an LWIR snapshot imaging spectropolarimeter,” *Proc. SPIE* **6295**, 62950E (2006).
15. R. W. Aumiller, N. Hagen, E. L. Dereniak, S. Robert, and R. McMillan, “New grating designs for a CTIS imaging spectrometer,” *Proc. SPIE* **6565**, 62950E (2007).
16. M. R. Descour, C. E. Volin, T. M. Gleeson, E. L. Dereniak, M. F. Hopkins, D. W. Wilson, and P. D. Maker, “Demonstration of a computed-tomography imaging spectrometer using a computer-generated hologram disperser,” *Appl. Opt.* **36**, 3694–3698 (1997).
17. J. P. Garcia and E. L. Dereniak, “Mixed-expectation image-reconstruction technique,” *Appl. Opt.* **38**, 3745–3748 (1999).
18. M. R. Descour and E. L. Dereniak, “Computed-tomography imaging spectrometer: experimental calibration and reconstruction results,” *Appl. Opt.* **34**, 4817–4826 (1995).
19. W. R. Johnson, E. K. Hege, D. O’Connell, and E. L. Dereniak, “Novel calibration recovery technique for an EM tomographic reconstruction,” *Opt. Eng.* **43**, 10–11 (2004).
20. C. E. Volin, J. P. Garcia, E. L. Dereniak, M. R. Descour, D. T. Sass, and C. G. Simi, “MWIR computed tomography imaging spectrometer: calibration and imaging experiments,” *Proc. SPIE* **3753**, 192–202 (1999).
21. C. E. Volin, “Portable snapshot imaging spectrometer,” Ph.D. dissertation (University of Arizona, 2000).
22. R. A. Horn and C. R. Johnson, *Topics in Matrix Analysis* (Cambridge U. Press, 1994).
23. W. H. Press, B. P. Flannery, S. A. Teukolsky, and W. T. Vetterling, “Sherman-Morrison and Woodbury formulas,” in *Numerical Recipes: The Art of Scientific Computing* (Cambridge U. Press, 1986), pp. 66–68.
24. P. J. Davis, *Circulant Matrices* (Chelsea, 1994).